

Analysis of the influence of Zn excess in the pineal gland by Total Reflection X-ray Fluorescence

1 Abstract

2 The TXRF technique (total reflection X-ray fluorescence) was employed to analyze the
3 concentration of zinc (Zn) and other metals in the pineal gland of rats submitted to orally
4 administered excess dose of Zn sulfate. The histochemical localization of Zn was also
5 performed. TXRF results showed a 42.9% increase in Zn concentration, and alterations on the
6 homeostasis of other essential elements in rats. It was concluded that TXRF is a suitable
7 technique for measuring, for the first time in this work, the concentration of Zn accumulated in
8 the pineal gland after administration of an excess dose of Zn , and this result may be either
9 directly or indirectly related to alteration in the homeostasis of other chemical elements , such
10 as S, Cl, K, Ca, Ti, Cr, Mn and Fe.

11 Keywords: Pineal, Rat, Zinc, TXRF, Hyperzincemia

12

13 Article highlights:

14 The X-Ray Fluorescence measured for the first time in the pineal the effects of excess
15 zinc on the homeostasis of trace elements.

16 The excess of zinc altered the homeostasis of S, Cl, K, Ca, Ti, Cr, Mn, Fe, increasing
17 these elements in the pineal.

18 Zinc histochemical techniques showed that after the overdose occurred important
19 changes in the pineal parenchyma.

20

21 Introduction

22

23 The pineal gland (PG, *epiphyse cerebri*) [1-5] is a neuroendocrine gland that integrates the
24 circumventricular organs; PG parenchyma is mainly composed of pinealocytes, microglia and
25 astrocytes [6]. The pinealocytes secrete melatonin, a neurohormone that is synthesized and
26 secreted almost entirely at night. Among other important functions, melatonin affects the
27 functioning of other important glands (such as the thyroid, adrenal, and gonads) and it can
28 modulate the bioavailability of zinc (Zn) in the plasma [1,7].

29 Metals perform many important physiological functions in the human body. The Zn oligo-
30 metallic ion is one of the most common and essential elements involved in brain function, and
31 it plays an important role in physiological and pathophysiological processes [8-9].

32 Zn is highly concentrated in the synaptic vesicles of subsets of glutamatergic neurons in some
33 brain regions, being particularly abundant in the hippocampus, amygdala, cerebral cortex,
34 thalamus, and olfactory bulb [10]. After iron (Fe), Zn is one of the most abundant D-block
35 metal [11-14] and is essential for several biochemical processes such as the control of cell
36 proliferation, myelination, and degeneration and serving to structural, catalytic, and regulatory
37 functions, protection against reactive oxygen species (ROS) and it is thought to play a role as a
38 neuromodulator [14-17] besides that, Zn and Fe play a pivotal role during neurodevelopment
39 and mediate cognitive development [18]. Zn is especially important in the immune system
40 because it plays a role as a molecular signal to, immune cells that are involved in the expression
41 of inflammatory cytokines and yet, several transcription factors need Zn to bind directly to
42 specific regions of DNA [19]

43 The multi-elemental composition of the human brain is important to its physiological function,
44 however, the distribution of elements in different tissues is not uniform, and some structures
45 can be the site of accumulation of toxic metals leading to multi-directional intracellular damage
46 principally in the central nervous system (CNS) where these disorders are especially dangerous
47 [20-21]. Zn concentration in the brains of both rats and humans increase after birth and remain
48 relatively steady throughout adult life [20]. In general, with respect to the total metal
49 concentration, the brain should possess efficient homeostatic mechanisms that prevent
50 abnormally high concentrations of metallic ions. Despite the important physiological role of Zn
51 in modulating several CNS functions, substantial evidence suggests that high concentrations of
52 Zn in the CNS can be neurotoxic [21-23]. Based on *in vitro* studies (in cortical cell culture) the
53 amount of Zn released during neurotransmission (~225-600 μM) depending of time exposition
54 is more than sufficient to cause fast neurotoxic effects [23-24].

55 Research on various brain diseases has indicated that trace metals such as Fe, Zn, copper (Cu),
56 and manganese (Mn) are key neurochemicals in the neuropathology of diseases and the
57 alteration of homeostatic mechanisms in CNS should lead to neurodegenerative disorders [25-
58 26]. The neurodegenerative disorders in which these metals [27-30] are implicated are all
59 characterized by a failure to maintain homeostasis, for example, the anomalous accumulation of
60 weakly bound Zn deposits that have been observed in senile plaques in the brains of
61 Alzheimer's patients [27-30]. The association of Zn (and Cu) to amyloid- β in Alzheimer's
62 disease suggests a central role in the abnormal metabolism of these metals in the pathology of
63 this disease. Then, metals dyshomeostasis has been linked to a variety of neurological
64 disorders, and it was found that inappropriate distribution of trace elements, as well as the

65 accumulation of toxic elements in structures of the human brain, is associated with the
66 occurrence of neurodegenerative diseases [28-30].

67 Total reflection X-ray fluorescence (TXRF) is a variant of Energy Dispersive X-Ray
68 Fluorescence (EDXRF) and is a multi-element technique. One of the major advantages
69 of this technique is the small sample amount required, a few microliters of a liquid or
70 micrograms of a solid. . In the case of solid samples, after the chemical digestion, a thin film is
71 formed in the sample carrier, and the effects of absorption and enhancement can be neglected
72 which simplifies the quantitative analysis [31]. In general, TXRF quantifications are performed
73 using the internal standardization method which involves the addition of an element that is not
74 present in the sample, for example, gallium (Ga). Internal standardization is useful because the
75 thin film formed on the Perspex sample support does not have a regular geometry and the X-
76 ray intensity depends on its position [32]. This geometry effect can be corrected by
77 normalizing each element's X-ray line to the internal standard added to each sample and
78 standard. Therefore, in contrast to conventional X-ray fluorescence (XRF), the concentration in
79 TXRF is simply determined by the relationship between the intensity of the radiation emitted
80 by the sample and the relative sensitivity of the system, which is determined using an internal
81 standard as described elsewhere [32]. This technique (TXRF) appeared to be suitable for the
82 present study because the pineal gland of rats young adult females are very small samples.

83 In an earlier study [2] we demonstrated that adult female rats treated with excess zinc
84 experienced severe changes in their motor behavior; this dose used was considered as a high
85 dose of zinc and inclusive capable of producing hyperzincemia and amyloidosis. In the present
86 study we focus on the potential role of induced hyperzincemia in female rats that received this large
87 oral doses of zinc relative to female rats of the same age and, untreated with Zn. The main
88 objective would be to evaluate the role of excess Zn in pineal histology, including revealing the
89 zinc in pineal tissue by means of specific methods for this ion [33-38]. The technique of TXRF
90 seemed quite adequate for the present study to quantify the amount of Zn in the pineal of the
91 female rats that received the oral doses of excess zinc, as well as, evaluate the potential role of
92 induced hyperzincemia in a possible one disruption of homeostasis of few other metals [31]
93 which are also quantified by TXRF.

94

95 **Methodology**

96 **Animals and Administration of oral doses**

97 Female Wistar rats (n=48) at postnatal (PN) day 90 (birth was considered PN 0) obtained from
 98 different colonies were kept in biological cages under normal laboratory conditions (12/12 h
 99 light/dark cycle) with water provided *ad libitum* and controlled food. These cages were doubles
 100 (with internal separation) allowing each rat to be isolated in its compartment. The rats were put
 101 in these cages a week prior to the postnatal age 90, with the aim to ambient them in these cages.
 102 All rats were weighed before (increased weight), during, and after the experiment (mean final
 103 weight = 188 g)

104 The animals were divided into three groups: two control groups (CG and NCG) and an
 105 experimental group (EG). The experimental group (EG) received zinc sulfate (ZnSO₄ solution
 106 0.1M, Sigma), one control group (CG) received sterile buffered saline, and the other control
 107 group (NCG) did not receive any solution.

108 The total dose of hyperzincemia] given [2] corresponded to 600 mg/kg of ZnSO₄ solution and
 109 was administered as follows: The dose was divided into 10 sub-doses being administered 1 sub-
 110 dose/day of ZnSO₄ solution (or the corresponding volume of saline solution); each rat received
 111 10 sub-doses which were administered as daily oral dose over a ten-day period, always
 112 administered without previous anesthesia and in the morning (~10:00 h), using a gavage needle
 113 for rats (diameter = 1,2 with ball) embedded in glycerin, in accordance with the norms and
 114 procedures from Experimental Ethics¹. Forty-eight hours after the administration of the last
 115 dose, the rats were killed by deep anesthesia (ketamine, xylazine, and acepromazine solution)
 116 and intracardiac perfusion. All protocols used for the animals were conducted in accordance
 117 with the Guide for the Care and Use of Laboratory Animals and were approved by the
 118 appropriate commission¹. The distribution of animals by technique is seen in Table 1.

119 The NCG used for the TXRF technique served to analyze whether the saline solution
 120 administered in the control group would change the concentration of chemical elements in
 121 biological samples.

122

123 **Table 1** Techniques and Number of rats and slides.

124

Techniques	Animals/ group		
	EG	CG	NCG

³ Comissão de Ética no Uso de Animais em Experimentação Científica (CEUA) do Centro de Ciências da Saúde da , Universidade Federal do Rio de Janeiro, under protocol number: **DAHEICB094-07/16 (year: 2013)**

125	Optical and fluorescence analysis and electron microscopy analysis (material embedding in Epon/Araldite)	11	11	4
126				
127				
128				
129	TXRF	9	9	4
130				
131	Slides /group and sections/slides			
132	TSQ	06/rat 4 sections/slide	06/rat 4 sections/slide	06/rat 4 sections/slide
133				
134	NEO-TIMM	10 /rat 6 sections/slide	10 /rat 6 sections/slide	10 /rat 6 sections/slide
135				
136				

137

138

139 **Histological methods and indicators for zinc**

140 Two techniques were used for zinc labeling to observation by optical microscopy: the Neo-
 141 Timm histochemical method (NTm) and the TSQ method (6-methoxy-8-quinolyl-
 142 *paratoluenesulfonamide*) (TSQm) [34-38]. The Neo-Timm has high selectivity to Zn and is the
 143 most used method to detect heavy metals in the mammalian brain [38]. The NTm is based on
 144 the conversion of the metal ion in the tissue into metal sulfide molecules, upon which the
 145 metallic silver is deposited.

²Riviera, E.A.B. Ética, bem-estar e legislação. In: Manual para Técnicos em Bioterismo. 2nd Ed. São Paulo, EPM, 1996.³ Comissão de Ética no Uso de Animais em Experimentação Científica (CEUA) do Centro de Ciências da Saúdeda , Universidade Federal do Rio de Janeiro, under protocol number: **DAHEICB094-07/16 (year: 2013)**

146 In this way, after the incubation of the sections in the developer solution, black precipitates of
 147 silver-metallic precipitates appear and mark the location of the zinc sulfide [36,38]. The TSQ
 148 **histochemical method** exhibits **blue fluorescence for free zinc or weakly bound** one [37].

149 For NTm was administered during the perfusion of rats a 0.9% saline solution (buffered PBS
 150 0.1 M) followed by 5 mL of sodium sulfide solution (Na₂S/Sorensen's buffer 0.15M, pH 7.4)
 151 for 10 minutes. and then 3% glutaraldehyde (in 0.15 M Sorensen buffer pH 7.4) for 3 minutes.

152 Then the same sodium sulfide solution was passed again for 7 min. The brains
 153 containing the pineal glands were removed, post-fixed in glutaraldehyde 3% (~ 1h); the pineal

154 glands were removed from the brain, oriented to obtain parasagittal sections and processed for
155 paraffin embedding.

156 The blocks were cut into 5- μ m sections (Rotary Microtome, Lipshaw) and sections (table 1)
157 were mounted on gelatinized slides. The slides were treated using the Neo-Timm method
158 simplified, as described in the literature [36,38]. histological preparations were deparaffinized
159 and hydrated and were placed in the developer solution (gum Arabic, citrate buffer,
160 hydroquinone, and silver nitrate) for 60 min (in the dark) and passed in 5% sodium thiosulfate
161 solution to stop the developer process. The histological preparations were counterstained with
162 hematoxylin [39]—dehydrated, clarified in xylene, and then mounted with Entellan (GTIN8
163 /EtellanMerck).

164 As for TSQm, [37] we used the non-fixed pineal glands; the glands were cryoprotected in
165 sucrose (10%, 20%, and 30%) overnight, soaked in OCT (optimum cutting temperature Tissue
166 Tek) and placed in this same medium. The blocks were sectioned in a cryostat (14 μ m thick)
167 (Slee Cryostal) at -14°C, and the sections were collected (Table 1) on gelatinized slides that
168 were then immersed (for 60 s) in the TSQ solution (4.5 μ M) buffered (140 mM barbital buffer
169 and 140 mM sodium acetate buffer, pH 10.5 – 11) and after incubation, were washed with 0,9%
170 saline. The material was analyzed using a fluorescence microscope with an ultraviolet filter
171 (Zeiss, excitation at 355-375 nm; dichroic mirror, 380 nm; barrier, 420 nm). The dithizone
172 method was used as a detection control. Dithizone [33] specifically removes zinc from tissues
173 and prevents TSQ detection. The sections were immersed in 10 mM dithizone for 5 min at
174 room temperature. After a 60 s immersion in TSQ buffer solution, the samples were washed
175 with normal saline and examined for TSQ fluorescence.

176 For electron microscopy, the rats were deeply anesthetized, as explained above, perfused
177 intracardially with 0.9% saline solution in 0,1 M phosphate buffer (PBS 0.1 M) followed by
178 4% paraformaldehyde fixative solution and 4% glutaraldehyde solution in 0,1 M phosphate
179 buffer. The brains were removed and post-fixed for 24h in the same fixative. The pineal glands
180 were removed and placed in 0.1 M phosphate buffer PBS. The material was embedded in pure
181 Epon for 72 h in a 60°C oven for polymerization and analyzed by electron microscopy (Zeiss
182 900 transmission electron microscope, Laboratory of Protozoan Biology UFRJ).

183 **TXRF analysis: sample and standard preparation**

184 The relative sensitivity of this technique for different elements can be calculated using multi-
185 element standard solutions. These standard solutions were prepared with varying and well-
186 known concentrations and contained Al, Si, K, Ca, Ti, Cr, Fe, Ni, Zn, Ga, Se, Sr, and Mo for

187 the K series (Table 2). Gallium (Ga) was also added as an internal standard for all the
188 multielement standard solutions and samples. The TXRF technique was used according to the
189 protocols cited in the literature [31,40,41] and summarized here: animals were sacrificed via
190 decapitation and their brains were quickly and carefully removed and frozen with liquid
191 nitrogen. The pineal glands were dissected and maintained at -70°C until the experiments were
192 performed. The feces from each animal were collected before, during, and after the
193 administration of the 10 doses (total of 3 samples per animal), were weighed, and subjected to
194 chemical digestion (in a stove) by adding nitric acid (HNO_3 - 65%) over 2 h, at 60°C . After the
195 chemical digestion, the volume of the samples was adjusted with deionized water and Gallium
196 solution to a final volume (μL).

197 The blood from each animal, collected at the time of the perfusion, was centrifuged (2,500 rpm
198 for 15 minutes) and 200 μL of serum was removed from each sample. For blood serum without
199 acid digestion, the volume of 200 μL was adjusted in the same way. The pineal from the EG,
200 CG and NCG were individually weighed (as a single sample for each group) to provide three
201 samples (EG = 3 mg; CG = 3.3 mg; NCG=3.3 mg) and the samples were submitted to chemical
202 digestion adding nitric acid (HNO_3 - 65%). After dissolution, the samples were mixed with a
203 gallium standard solution (102.5 ppm). All samples (including the blood serum samples) were
204 prepared in duplicate to provide better results. Blank samples (only water, gallium and HNO_3)
205 were prepared to evaluate any source of contamination (without nitric acid for the blood
206 serum). Small amounts (5 μL) of the final solutions were pipetted onto a clean Perspex sample
207 support (lucite), and each sample was dried under infrared light. To create the calibration curve,
208 standard solutions containing the chemical elements (Table 2, Fig. 1), for the K-lines, were
209 prepared in varying, well-known concentrations, with gallium as the internal standard. The
210 TXRF measurements were performed at the D09-B beamline from the Brazil Light
211 Synchrotron Laboratory in Campinas, São Paulo, Brazil. The sample carrier was placed in a
212 horizontal plane relative to the hyper-pure germanium (HPGe) detector (resolution 140 eV at
213 5.9 KeV), which was positioned perpendicularly to the sample carrier, and excited with a white
214 beam of synchrotron light with a maximum energy of 20 keV and filtered by 0.5 mm of
215 aluminum (with an incidence angle of 1.0 mrad). The sample and standards were excited for 100
216 s. The X-ray spectra obtained were evaluated using Quantitative X-ray Analysis System
217 (QXAS) software which is distributed by the International Atomic Energy Agency (IAEA), to
218 obtain the X-ray intensities and associated uncertainty for each element. The fluorescence
219 intensities were obtained by fitting the spectra to the QXAS.

220

221 **TABLE 2.** Multielemental standard solution concentrations (mg/L) were used for the
 222 calibration of the system for the K series.

Element	1K	2K	3K	4K	5K	6K
Al	50	40.9	36.36	31.82	27.27	22.73
K	100	81.82	72.73	63.64	54.54	45.45
Ca	10	8.2	7.27	6.36	5.45	4.5
Cr	50	40.9	36.36	31.82	27.27	22.73
Mn	10	8.2	7.27	6.36	5.45	4.5
Fe	10	8.2	7.27	6.36	5.45	4.5
Co	10	8.2	7.27	6.36	5.45	4.5
Ni	50	40.9	36.36	31.82	27.27	22.73
Cu	10	8.2	7.27	6.36	5.45	4.5
Zn	10	8.2	7.27	6.36	5.45	4.5
Sr	10	8.2	7.27	6.36	5.45	4.5
Mo	50	40.9	36.36	31.82	27.27	22.73

223

224

225 **Insert Fig. 1**

226

227

228 **Statistical analysis**

229 The results were expressed as the mean values \pm the standard error, and the means were
 230 compared using an analysis of variance (ANOVA) with a 5% significance level. The
 231 means were also compared between groups using Tukey's test. All statistical analyses
 232 were performed using BioEstat 5.0 computer software (Free Statistics/www.freestatics.info).

233

234 **Results**

235 Using the TXRF technique we found that the pineal glands (EG) of animals receiving an excess
 236 dose of ZnSO₄ showed a 42.9% (150 $\mu\text{g}\cdot\text{g}^{-1}$) increase in zinc concentration relative to the control
 237 groups (CG and NCG) (Table 3). This increase may represent changes in zinc homeostasis.

238 The homeostatic balance of other chemical elements also changed in the PG under
 239 hyperzincemia conditions. The concentrations ($\mu\text{g}\cdot\text{g}^{-1}$) of S, Cl, K, Ca, Ti, Mn and Fe also
 240 increased relative to those of the PG of the control animals. However, the concentrations of P
 241 and Ni decreased ($\mu\text{g}\cdot\text{g}^{-1}$) (Table 3). It was not possible to analyze the concentration of copper
 242 (Cu) in the pineal gland because the values were below the limit of detectability. The excess
 243 administered zinc did not significantly alter the zinc concentration in the serum. However,
 244 alterations were observed in the serum concentrations of other elements. There was a
 245 statistically significant decrease in Fe concentration and a significant increase in the S, Cl,
 246 and K concentrations in the serum of animals that received zinc.

247

248 **Table 3** Percentage comparison of the concentrations of the chemical elements of the control
 249 group with those of the experimental group. The chemical elements are in ascending order
 250 according to their atomic number (Z).

Groups / Element	Pineal Gland Elemental Concentration ($\mu\text{g}\cdot\text{g}^{-1}$)			Blood Serum Elemental Concentration ($\mu\text{g}\cdot\text{ml}^{-1}$)		
	CG	EG	(%)	CG	EG	(%)
Si	52±0.67	89±36	-	<LMD	7±2	<LMD
P	8478±109 ^a	1404±62 ^a	83.44 D	15±6	14±6	-
S	1244±20 ^a	2215±23 ^a	78.10 I	40±8 ^a	62±18 ^a	55 I
Cl	864±26 ^a	1736±22 ^a	101 I	218±91 ^a	290±72 ^a	33 I
K	2893±8 ^a	4040±43 ^a	39.66 I	281±54 ^a	491±88 ^a	74.7 I
Ca	1835±17 ^a	4272±56 ^a	132.80 I	228±118	221±123	-
Ti	43±4 ^a	62±6 ^a	44.20 I	7±2	9±3	-
Cr	29±1	28.8±5	-	4±2	4±2	-
Mn	3.5±0.6 ^a	6.0±0.85 ^a	71.44 I	0.9±0.2	1.5±1	-
Fe	645±11 ^a	1953±26 ^a	202.8 I	348±173 ^a	245±96 ^a	29.6 D
Ni	100±0.78 ^a	47±0.5 ^a	53 D	2±1	4±2	-
Zn	105±0.5 ^a	150±1 ^a	42.90 I	13±5	13±4	-

251 Values are the means ± standard error. (a) indicates statistically significant differences among
 252 the groups at $P \leq 0.05$; LMD, minimum detectable value; concentrations (%); I, increase; D,
 253 decrease.

254

255 Analysis of pineal parenchyma using electron microscopy showed disorganized fibrillar
 256 depositions and alterations in the blood vessels walls that appeared thinner and smoother and
 257 with imperfections in experimental animals (EG) (Fig. 2B) in relation to the control groups
 258 (Fig.2A). The pineal gland's parenchyma in the EG evidenced that the excess zinc disrupted

259 the normal architecture and this was particularly visible with respect to the wall of the blood
260 vessels and enlarged peripheral spaces (Fig.2B; white stars). In rats' controls, the
261 parenchyma was more homogeneous and had a well-defined structure of blood vessels with
262 fingerlike projections (Fig. 2A and insert) characteristic of normal pineal vessels. These
263 fingerlike projections were modified in the EG (Fig. 2B; black arrows), where some degree of
264 disorganization was apparent in the periphery of the blood vessel (Fig. 2B; white arrows), and
265 there was a noticeable decrease in the vessel wall thickness in EG rats (Fig. 2B). In rats of CG
266 (Fig. 3 A) the pineal blood vessels stained by hematoxylin and eosin showed a regular
267 organization and the parenchyma was more organized as compared to the experimental group
268 (Fig. 3C and insert). The Neo-Timm method revealed Zn deposits (zinc aggregates in black)

269

270

Insert Fig. 2

271

272 adjacent to blood vessels (Fig. 3B, a) in the pineal gland. These deposits appeared in larger
273 quantities in the experimental group than in the controls (not shown here) (EG 161 aggregates;
274 CG = 64 aggregates; NCG = 65 aggregates). In figure 3C, the arrows show the significant
275 disruptions in relation to the blood vessel walls, and it is possible to observe a decrease in
276 thickness in these walls. The TSQ method produced an intense bright blue fluorescence (Fig.
277 4A) that was brightest in the pseudorosette (Fig. 4A, demarcated area) cellular arrangements
278 around blood vessels [4] and in the pineal cells scattered throughout the parenchyma. In the
279 control groups (Fig. 4B) the fluorescence was less evident, and this weak fluorescence
280 perceived is considered to represent the location of zinc that normally exists in tissue.

281

282

Insert FIG. 3 and Fig. 4

283

284

285 Discussion

286 The present study quantified Zn in the pineal gland by the TXRF technique [41]. This technique
287 was required because the pineal gland is small and thus provides a very limited sample for
288 analysis. By using TXRF, we were able to obtain significant quantitative information, even
289 with the small amount of tissue available, from animals administered with excess Zn. It is
290 important to note that this type of sensitive quantification of pineal gland samples had never
291 been achieved, particularly under conditions where an excess of Zn was administered. Zn is an
292 essential trace element that is normally present in small amounts in the body [42]. However,

293 high concentrations may accumulate in the cerebral cortex and hippocampus and can have toxic
294 effects, as observed in neurons cultured from mice exposed to increased Zn concentrations
295 [43,44]. In Alzheimer's disease [45] metals such as Zn and Cu favor the aggregation of β -
296 amyloid peptides and can be histochemically detected in the amyloid deposits of senile plaques.
297 Despite evidence of the toxic effects of Zn, the literature provides more information on the
298 consequences of Zn deficiency (hypozincemia) than that of Zn excess (hyperzincemia) [46].
299 For example, Zn deficiency, besides Cu overload, has been identified as a risk factor for autism
300 spectrum disorders (ASD) [47].

301 According to our results (Table 3) by TXRF, there was an increase (42.9%) in Zn concentration
302 in the pineal gland after excess Zn administration, which allows us to infer that the pineal gland
303 is a target for Zn accumulation. This finding is strengthened by evidence that higher levels of
304 Zn were found in the pineal gland [48] of some animals (calves, cows and pigs) [49].
305 Particularly, in the human pineal gland and in some brain tumors it has been reported a
306 beneficial association between high zinc content and specific physiological roles [6, 49,
307 50,51,52]. In mammalian cells approximately 98% of the total Zn concentration in the body is
308 intracellular, and only a small portion accumulates in the extracellular matrix. Neurons
309 containing "free ionic zinc" (Zn^{2+}) are found in various areas of the brain, including the cortex,
310 amygdala, olfactory bulb, and hippocampal neurons, pineal, which appear to have the highest
311 concentration of zinc in the brain [9,10,51,52]. The intracellular homeostasis of Zn is
312 regulated by membrane importers and exporters, known as zinc carriers and these are divided
313 into two distinct families: the ZIP and ZnT families [42, 52,53, 54,55,56]. ZIP transporters
314 mediate the influx of Zn into the cytoplasm, resulting in an increased level of intracellular zinc:
315 the ZnT family acts to reduce intracellular zinc by promoting its efflux from cells or
316 intracellular vesicles [57-59].

317 Zn homeostasis is also regulated by the intracellular Zn storage protein, metallothionein (MT)
318 which readjusts the intracellular stock and maintains ion homeostasis [49, 60,61,6 2,63,64].
319 MT acts as a scavenger when Zn is present in high concentrations, as well as a zinc reservoir to
320 supply Zn when it is deficient. Zinc homeostasis is essential for cellular events and its
321 dysfunction can lead to several human disorders [65,66]. In humans, the main mechanisms
322 regulating zinc homeostasis are absorption and excretion, and organs such as the small
323 intestine, pancreas, and liver play central roles in its maintenance [60,65]. In these organs,
324 transepithelial transport refers to the transfer of metals across the apical and basolateral
325 membranes to be picked up and distributed by soluble transporters [69] The transepithelial zinc
326 movement is orchestrated by many mammalian zinc transporters specialized for selective

327 capture, and movements of Zn ions across the membrane barrier that depend on an
328 electrochemical gradient, for instance, the bacterial zinc acquisition depends on ZIPB
329 transporter zinc in an opposite direction, down a zinc concentration gradient [58,66]. Zinc
330 fluxes across apical and basolateral membranes need to be balanced and the abundance of ZIP4
331 and ZnT1 on the respective cell surfaces is tightly regulated according to the Zn availability.
332 The high extracellular Zn levels induce internalization of surfaced ZIP4, as well as promote the
333 drastic removal of cellular ZIP4 via proteasomal and lysosomal degradation pathways [67-71].
334 In mice and rats fed with a diet containing Zn, ZIP4 is hardly detected -but a detailed analysis of
335 the mouse and rat and human differences in the kinetics of endocytosis and degradation of ZIP4
336 is required, to gain a more complete understanding of the regulated ZIP4 and their underlying
337 mechanisms of endocytosis in mammals [70]. When Zn is orally administered it is absorbed
338 (20-30% of the ingested content) by the gastrointestinal tract through both active (saturable)
339 and passive (diffusion). Zinc uptake takes place on the intestinal brush border membrane of the
340 enterocytes transport. After ingestion and absorption, there is a vectorial Zn movement from the
341 intestinal lumen to the blood. The excretion of Zn on the basolateral side of the enterocytes
342 releases it into the portal blood, where it is predominantly bound to albumin, which distributes
343 the metal in the body. In general, absorption of Zn is promoted through the presence of small
344 molecular compounds (amino acids and hydroxy acids and animal proteins [68-72].

345 The role of metallothionein (MT) [73,74] is to bind zinc with high affinity and to serve as an
346 intracellular zinc reservoir. When needed the MT can release free intracellular zinc. MT
347 expression is induced by zinc elevation, and thus, zinc homeostasis is maintained.
348 Notwithstanding, there is a critical period (CP) of 6 to 12 days [75] for the homeostatic
349 regulation of Zn in plasma, and recovery from the effects of either hypozincemia or
350 hyperzincemia. A study using ⁶⁵Zn showed considerable variation in Zn elimination from
351 different brain regions in rats with half-lives ranging from 16 to 43 days [64]. During the CP,
352 metallothionein (MTs) play a role as metabolic zinc-binding proteins and are capable of
353 regulating Zn bioavailability, preventing alterations in ion concentrations from disturbing
354 homeostasis[] For the pineal gland discussed in this paper, we do have not enough
355 information on the transport mechanisms of Zn, and the activity of the metallothioneins to
356 discuss our results about Zn drive after ingestion of this ion, although there is data suggesting
357 the presence of a metallothionein-I-II expression system in the pineal gland of bovines [49].
358 Although these proteins are involved in metal detoxification, the mechanism of this protection
359 is unclear. Therefore, it is impossible to clearly explain how the high amounts of Zn were

360 retained by the pineal gland of young rats exposed to an excess of Zn. In the same way, one
361 study evaluated the effect of zinc overdose (the ingestion of two different doses of zinc
362 chloride, ZnCl₂) on the homeostasis of metals (Mn, Cu, Fe and Zn) in the liver of rats, and
363 the results showed that this excess of ZnCl₂ causes an accumulation of these metals in the
364 liver when compared to controls [76]. Recent studies relate the difficulty to elucidating the
365 cellular transport systems for other trace elements when toxic, such as cadmium (Cd),
366 mediated by the transporter for manganese (Mn) and by members of the ZIP transporter family
367 (ZIP8 and ZIP14), identified in studies as transporters having high affinities for both Cd and
368 Mn[77].

369 According to the literature, the primary transportation route for Zn to the brain involves the
370 blood-brain barrier, and the choroid plexus may participate in the slow supply of Zn to the brain
371 and the blood-brain barrier maintains the homeostasis of the microenvironment regulating the
372 balance of zinc in the brain [78]. For this reason, the blood-brain barrier is important for Zn
373 homeostasis because disturbance to metal homeostasis is a common characteristic of
374 neurological dysfunction and neurodegenerative diseases [79, 80]. It has been reported that L-
375 histidine is involved in Zn transport into the brain through the blood-brain barrier via a divalent
376 metal transporter (DMT1) expressed in capillary endothelial cells and choroidal epithelial cells
377 in the brain. DMT1 is also involved in the transportation of other highly toxic cations trace
378 elements such as Pb²⁺, Cd²⁺, Co²⁺, Ni²⁺ and Pt²⁺ [81]. Another element for Zn²⁺ transport is
379 ZIP8, a member of the ZIP transporter family [82] principally involved in the transport of this
380 metal at renal tubules [82,83].

381 In the case of the pineal gland [84] that has strong blood circulation and there is no true blood-
382 brain barrier [2]. DMT1 is a transporter not cited in the pineal literature to date, as well as the
383 ZIP8; but the present study is inclined to consider that the accumulation of Zn in the pineal
384 gland might be favored by the absence of a blood-brain barrier in this gland. The fact that the
385 pineal has no blood-brain barrier and is highly vascularized by a capillary network organized
386 by the parenchyma, with its capillaries presenting fenestrations is a factor that implies in
387 exchanges of substances between tissues and vessels faster and easier [85,86]. The intrapineal
388 vascular architecture varies with specific features concerning the peripheral part, poorly
389 vascularized by small and fine blood vessels and, the central part of the gland highly
390 vascularized by large sinusoid capillaries [84- 86].

391 Although there is a relationship between melatonin (the primary product of the pineal gland)
392 [87] and the plasma zinc level, the analysis of any relationship between melatonin levels and
393 excess zinc was not the objective of this study, although it is important to evaluate this

394 relationship in the future, but considering that in the present study plasma zinc did not change
395 (Table 3).

396 Using the Neo-Timm and TSQ histological techniques, the present study demonstrated that Zn
397 is primarily accumulated in the perivascular space and appears as dark granules that reveal the
398 location of Zn deposits when tissues are treated with NTm. These aggregates near blood vessels
399 were more evident in rats orally treated with excess zinc (Fig. 3B). Unfortunately, in the
400 present study it was not possible to perform a more specific technique to determine the precise
401 location of these aggregates in the pineal blood vessel wall (Fig 3B), something that should be
402 done. The presence of Zn in the perivascular space was also histochemically reactive to TSQ
403 (diffuse fluorescence) (Fig. 4) in the rats treated with excess zinc (EG). TSQ is a dye that can
404 penetrate cellular membranes to stain both vesicular Zn and zinc that is only weakly bound to
405 proteins. Therefore, the material detected by TSQ in some cells and in the perivascular space of
406 the pineal gland may represent either types of zinc, and a possibility of this abnormal
407 accumulation could be due to changes in the Zn transport system of the endothelium, a
408 saturable system mediated by families of transporters (ZnT and Zip). These transporters are
409 regulated by the amount of Zn concentration. Even though the brain has strict regulatory
410 mechanisms that keep fluctuating concentrations of metals to prevent their shortage or excess,
411 which may be related to various neuropathies [30,45,54] very little is known about how the
412 potential system transport of Zn in the pineal responds to the accumulation of this ion.

413 TXRF analysis also indicated that the serum Zn concentration did not change significantly.
414 This result is not surprising because it is known that the concentration of Zn in serum is mostly
415 influenced by the circadian rhythm, with lower values in the morning (when the animals were
416 euthanized) and increased values in the afternoon [2]. To better understand why the Zn
417 concentration in the serum of rats did not change, the results obtained after 10 zinc doses were
418 compared with the Zn concentrations found in serum from the controls (CG and NCG) and
419 serum taken after administration of the first to fifth doses of Zn (D5). No changes occurred in
420 the Zn concentration in the serum. However, after D5, the rats were already experiencing
421 increased weakness, and it was more difficult to continue taking blood samples [2]. Thus, the
422 last blood sample was taken at D10 (before the addition of the fixative solution, during the
423 passage of saline solution) and the blood serum was collected and analyzed.

424 The resulting comparison verified that the Zn concentration in the serum remained virtually
425 constant at all analyzed times (Table 3), the values of CG and EG are very similar, with a very
426 small decrease in serum of EG animal after the 10 doses of zinc. Fecal samples collected from
427 the animals throughout the experiment also showed no significant changes in Zn concentration. It

428 is difficult to explain with certainty why there was such a small decrease in serum zinc in the
429 EG animal, if it was assumed that there was an overdose of Zn in the pineal cells after the 10
430 zinc sulfate doses.

431 Considering what was said before about the efflux of zinc out of the cell through the
432 membrane, one hypothesis could be some disturbance in the Zn transport system which
433 promotes its efflux. In addition to the increased concentration of Zn in the pineal gland,
434 statistically significant alterations were observed for the concentrations of other elements such
435 as S, Cl, K, Ca, Ti, Mn and Fe (Table 3). The relationship among the concentrations of various
436 chemical elements is essential for the proper functioning of the body, and alterations in the
437 concentration of some metals can affect the bioavailability of other essential metals [67]. This
438 is important because according to current knowledge it turns out that metals such as Na, K, Mg,
439 Ca, Fe, Mn, Co, Cu, Zn and Mo are essential elements for life and our body must have adequate
440 amounts of them.

441 Thus, it is important to quantify the correlation among chemical elemental concentrations as
442 done for some areas in the brains of Wistar rats of different ages by the TXRF method [31].

443 In the current study, the changes in the concentration of the other chemical elements were
444 also detected by TXRF (Table 3) and such changes could be either directly or indirectly linked
445 to the administration of excess zinc, but a discussion of these factors is beyond the scope of this
446 study. However, there are some remarkable aspects of our results, such as the >100% increase
447 in

448 the concentrations of certain ions (Table 3) such as Fe. In relation to iron (Fe), which is an
449 essential element for normal body functioning [80] its concentration in the pineal gland
450 increased significantly following the addition of excess zinc (Table 3). In general, a large
451 increase in iron concentration is harmful because it can promote the generation of toxic reactive
452 oxygen species (ROS) that can damage proteins, lipids, and DNA, and the irregular deposition
453 of iron is a common feature in some diseases. Studies of Fe and Zn interactions in neural
454 tissues are scarce but the literature suggests a biological (micronutrient status) interdependence
455 between iron and zinc in the brain [79]. Previous studies demonstrated an antagonism
456 between Fe and Zn, citing absorptive competition between iron and zinc at the receptor DMT1,
457 however, evidence showed that the DMT1 is not the primary intestinal transporter of zinc.
458 Moreover, there are well known evidence that excess Zn intake through diet or supplements,
459 can affect iron absorption: it has been shown that following the administration of Zn overdose it
460 is possible to detect an increase of Fe accumulation in the liver, suggesting a strong disturbance of
461 Zn homeostasis in this organ after overdose of zinc, and interference with iron metabolism. For

462 some authors, these increases and decreases in chemical elements after zinc excess intake, led
463 to the conclusion of a synergic relationship between Fe, Mn and Cu and Zn, but this
464 accumulation of Fe, for example, can determine an intensification of cell oxidative reactions
465 and an oxidative stress appearance [88].

466 Our results showed increased Fe concentration within the pineal gland in parallel to its
467 reduction (~ 30%) in the serum (Table 3); however, it is unclear why the increased Zn
468 concentration triggered an imbalance of iron, likewise that described to the overdose of $ZnCl_2$,
469 for instance [67].

470
471 Calcium can appear as free Ca^{2+} both extracellularly and intracellularly [89]. The increased
472 concentration and accumulation of Ca observed in the pineal gland by TXRF method (Table 3)
473 may be reflecting the Ca release from intracellular stores, such as those in the mitochondria or
474 endoplasmic reticulum [90]. There is evidence that Zn can increase the permeability of cell
475 membranes to Ca and thus contributing to homeostatic imbalance. Release of Ca from the
476 mitochondria may also occur because of changes in Mn concentration [90]

477 Mn may induce cellular damage through mitochondrial dysfunction and can release Ca from
478 intracellular stores under certain conditions [92]. In the current study, it was observed a
479 substantial increase in the concentration of Ca and Mn (Table 3). There are reports about an
480 excess of manganese which can cross the blood-brain barrier (BBB), and accumulate in some
481 regions of the brain (considering that pineal do not have BBB) thereby producing toxicity and
482 neuropathies [93]. Complementary studies are needed to determine whether these observed
483 changes in Ca and Mn homeostasis are interrelated.

484 **However, speculations** regarding these findings are beyond the scope of the present study.

485 An unexpected result was the reduced concentrations of phosphorus (P) and nickel (Ni)
486 observed in the pineal gland (but not in the serum) after the excess of Zn, a difficult result to
487 interpret. P in the body is in the form of phosphate, and phosphate has a reciprocal relationship
488 with Ca (a decrease in phosphate content implies an increase in Ca concentration) therefore, the
489 excess of one implies increased excretion of the other. It is possible that the changes in P are
490 more closely related to Ca than to excess of Zn.

491 Among the increased concentrations in the pineal gland of S (sulfur), Cl (chloro) and K
492 (potassium) (Table 3), and in the serum related to excess Zn, it is particularly important to note
493 the increase in K concentration. The high K concentration in the serum could be explained by a
494 sudden release of intracellular K reservoirs into the blood that exceeds the elimination capacity

495 of the kidneys, creating a potentially lethal condition [93]. The reason for the increased K
496 concentration into the blood following the administration of excess zinc requires further
497 investigation.

498 We also find it important to consider that rats subjected to a dosage of ZnSo₄ like that used in
499 this study showed decreased motor activity when tested in the open field maze after the 10
500 doses of zinc sulfate [2]. One hypothesis raised is that this response is due to the breakdown of
501 homeostasis of the various trace elements as analyzed in the present study, and this would be
502 corroborate previous studies [18] where changes in the homeostasis of Zn and other metals
503 would be implicated in the pathogenesis of certain diseases.

504

505

506 **Conclusions**

507 This study used the TXRF technique to demonstrate, for the first time, that the concentrations
508 of Zn and other essential elements (S, Cl, K, Ca, Ti, Mn, and Fe) in the pineal gland of young
509 rats increased considerably following the administration of excess zinc sulfate.

510 Further studies are needed to determine the factors involved in changing (the breakdown) the
511 homeostasis of Zn and these other chemical elements.

512 TXRF successfully quantified the elemental changes within this gland, thus proving to be an
513 effective, reliable, and efficient technique for quantifying chemical elements in small
514 samples such as the pineal gland. TXRF can be considered another important analytical
515 tool for the study of the mammalian pineal gland.

516 Although this study clearly showed alterations in ion homeostasis, further investigations are
517 needed to determine the mechanisms underlying such alterations and clarify the role of the
518 increased concentrations of these ions in the pineal gland, following the administration of
519 excess
520 zinc.

521 However, these results are sufficient to validate our suggested model of animal hyperzincemia
522 [2] where the animals showed a significant change in motor behavior after 10 doses of zinc

523 sulphate; in addition, irregular deposits of zinc appeared adjacent to pineal gland vessels, in the
524 same area occupied by amyloid deposits [2].

525 The present study contributes to the pineal literature because it shows, also for the first time, the
526 effect of an excess of zinc sulfate on trace elements homeostasis in female rat pineal gland.

527

528 **Ethical Approval:**

529

530 Animal Ethic committee approval has been collected and preserved by the author(s)

531

532 **Acknowledgments:**

533

534 Our thanks to Light Synchrotron Brazilian Laboratory for the use of

535 D09-B beam line. Our thanks to the Laboratory of Protozoan Biology,

536 Professor Paulo de Góes Microbiology Institute, UFRJ, for the use of the

537 electron microscope, kindly provided by Dra. Thais Cristina Baeta Soares

538 Souto-Pradón.

539

540 **References:**

541 1. Ekstrom P, Meissl H (2003) Evolution of photosensory pineal organs in new light:
542 the fate of neuroendocrine photoreceptors. *Phil Trans R Soc Lond B* 358:1679-1700.

543 2. Ferezin-Pinto C (2010) Investigações mineralógicas, histopatológicas e

544 Ultraestruturais usando o modelo experimental de hiperzincemia na glândula pineal de

545 ratas jovens. Tese de Mestrado, Universidade Federal do Rio de Janeiro (UFRJ),

546 Programa de Ciências Morfológicas do Instituto de Ciências Biomédicas, CCS, Rio de

547 Janeiro, Brasil.

548 3. Ferreira-Medeiros M, Correa-Gillieron EM (2004) Recognition of N-

549 acetylglucosamine and Poly-N-acetyl lactosamine residues in vessels of the rat pineal

550 gland. *Int J Morphol* 22:285-290.

551 4. Ferreira-Medeiros, Mandarim-de-Lacerda CA, Correa-Gillieron, EM (2007). Pineal

552 gland post-natal growth in rat revisited. *Anat Histol Embryol* 36(4): 284-289.

- 553 5. Reiter RJ (1981). Pineal melatonin : cell biology of its synthesis amd of its
554 physiological interactions..Endocr. Rev. 12:151-180.
- 555 6. Bukreeva I, Junemann O, Cedola A, Palermo F, Maugeri L, Provinciali GB, Pieroni
556 N, Sanna A, Otylga DA, , Buzmakov A, Krivonosov Y, Zolotov D, Chukalina M,
557 Ivanova A, Saveliev S, Asadchikov V, Fratini M (2020) Investigation of the human
558 pineal gland 3D organization by X-ray phase contrast tomography. Journal of Structural
559 Biology 212:1-12.
- 560 7. Opresko DM (1992) Toxicity summary for zinc and zinc compounds, Chemical
561 Hazard Evaluation and Communication Group Biomedical and Environmental
562 Information Analysis Section, Health and Safety Research Division – Prepared for Oak
563 Rdge Reservation Environmental Restoration Program, Oak Ridge, Tennessee
- 564 8. Brito S, Lee MG, Bin BH, Lee JS (2020) Zinc Homeostasis Regulates Epigenetics.
565 Mol. Cells 43(4): 323-330.
- 566 9. Choi S, Hong Dk, Choi B, Suh SW (2020) Zinc in the Brain: Friend or Foe? Int J
567 Mol Sci 21(23) 8941: 1-24.
- 568 10. Blakemore LJ, Trombley, PQ (2017) Zinc as a Neuromodulator in the Central Nervous
569 System with a Focus on the Olfactory Bulb. Frontiers in cellular neuroscience 297:1-20.
- 570 11. Constable EC (2019) Evolution and understanding of the d-block elements in the periodic
571 table. Royal Society of Chemistry. Dalton Trans. 48, 9408-9421.
- 572 12. Bitanirwe, BK, Cunningham, MG. (2009) Zinc: the brain’s dark horse. Synapse
573 63:1029–1049.
- 574 13. Ozturk G, Akbulut KG, Afrasyap L (2008) Age-related changes in tissue and
575 Plasma Zinc levels: modulation by exogenously administered melatonin. Exp Aging Res
576 34:453-462.
- 577 14. Frederickson CJ, Sang Won Suh, DS, Frederickson CJ, Thompson RB (2000) Importance of
578 Zinc in the Central Nervous System: The Zinc-Containing Neuron, The Journal of Nutrition, v:
579 130, Issue 5: 1471S–1483S, <https://doi.org/10.1093/jn/130.5.1471S>
- 580 15. López-García C, Varea E, Palop JJ, Nacher J, Ramirez C, Ponsoda X, Molowny A
581 (2002) Cytochemical techniques for zinc and heavy metals localization in nerve cells.
582 Microsc Res Tech 1,56(5):318-31.
- 583 16. Janssen CR, De Schamphelaere K, Heijerick D, Muysen B, Lock K, Bossuyt B,
584 Vangheluwe M, Sprang P (2000) Uncertainties in the environmental risk assessment of
585 metals. Hum Ecol Risk Assess 6:1003-1018.
- 586 17. Poweel SRA (2000) The antioxidant properties of zinc. J. Nutr. 130:1447-1454.

- 587 18. de Moura, JE, de Moura, ENO, Alves, CX, Vale SHL, Dantas, MMG, Silva, AA, Almeida
588 MG, Leite, LD, Brandão-Neto, J (2013). Oral Zinc Supplementation May Improve Cognitive
589 Function in Schoolchildren. *Biol Trace Elem Res* 155, 23-28.
590 <https://doi.org/10.1007/s12011-013-9766-9>
- 591 19. Wessels, I, Maywald, M, Rink, L (2017). Zinc as a Gatekeeper of Immune
592 Function. *Nutrients*, 9(12), 1286. <https://doi.org/10.3390/nu9121286>
- 593 20 . Jarosz M, Olbert M, Wyszogrodzka G, Mlyniec K, Librowski T (2017) Antioxidant
594 and anti-inflammatory effects of zinc. Zinc-dependent NF-kappaB signaling.
595 *Inflammopharmacol* 25:11–24.
- 596 21. Bitanhirwe, BK, Cunningham, MG. (2009) Zinc: the brain's dark horse. *Synapse*
597 63:1029–1049.
- 598 22. Campbell A, Smith MA, Sayre LM, Bondy SC, Perry G (2001) Mechanisms by which
599 metals promote events connected to neurodegenerative diseases. *Brain Resear Bull*
600 55:125-132.
- 601 23. Bush AI (2000) Metals and neuroscience. *Curr Opin Chem Biol* 4:184-191.
- 602 24. Choi DW, Yokoyama M, Koh J (1988) Zinc neurotoxicity in cortical cell culture.
603 *Neuroscience*. 24(1):67-79. doi: 10.1016/0306-4522(88)90312-0.
- 604 25. Kawahara, M, Kato-Negishi, M, Tanaka, KI (2020). Amyloids: Regulators of metal
605 homeostasis in the synapse. *Molecules*, 25(6):1441-1460.
- 606 26. Cuajungco MP, Less G (1997) Zinc metabolism in the brain: relevance to human
607 neurodegenerative disorders. *Neurobiol Dis* 4:137-169.
- 608 27. Bush AI, Pettingell WH, Multhaup G, Paradis M, Vonsattel JP, Gusella JF,
609 Beyreuther K, Masters CL, Tanzi RE (1994) Rapid induction of Alzheimer A beta
610 amyloid formation by zinc. *Science* 265:1464-1467.
- 611 28. Erikson, K. M., Thompson, K., Aschner, J., & Aschner, M. (2007). Manganese neurotoxicity: a
612 focus on the neonate. *Pharmacology & therapeutics*, 113(2), 369–77.
613 doi:10.1016/j.pharmthera.2006.09.002.
- 614 29. Koh JY, Suh SW, Gwag BJ, He YY, Hsu CY, Choi DW (1996). The role of zinc in
615 selective neuronal death after transient global cerebral ischemia. *Sci*. 272: 1013-1016.
- 616 30. Adlard PA, Bush, AI (2018) Metals and Alzheimer's disease: How far have we come
617 in the clinic? *J. Alzheimers. Dis* 62:1369–1379.
- 618 31. Serpa RFB, Jesus EFO, Anjos MJ, Carmo MGT, Moreira S, Rocha MS, Martinez
619 AMP, Lopes RT (2006) Elemental concentration analyze in brain structures from
620 young, adult and old Wistar rats by total reflection X-ray fluorescence with synchrotron

- 621 radiation. *Spectrochim Acta Part B* 61:1205-1209.
- 622 32. Klockenkamper R. (1996) Total-Reflection X-Ray Fluorescence Analysis. Institut
623 fur Spectrochemie und Angewandte Spektroskopie. v. 140. Dourtmund, Germany.
- 624 33. Shaw E, Dean LA (1952) Use of Dithizone as an extractant to estimate the zinc
625 Nutrient. Status of soils. *Soil Sci* 73(5):341-348.
- 626 34. Hamani C, de Paulo I, Mello LEAM (2005) Neo-Timm staining in the thalamus of
627 chronically epileptic rats. *Braz J Med Biol Res* 38:1677-1682.
- 628 35. Danscher G (1981) Histochemical demonstration of heavy metais. *Histochemi* 71:1-
629 16.
- 630 36. Danscher G, Zimmer J (1978) An improved Timm sulphide silver method for light
631 and electron microscopic localization of heavy metals in biological tissue. *Histochemi*
632 55:27-40.
- 633 37. Frederickson CJ, Kasarkis EJ, Ringo D, Frederickson RE (1987) A quinoline fluorescence
634 method for visualizing and assaying the histochemically reactive zinc (bouton zinc) in the
635 brain. *J. Neurosci. Methods* 20:91-103.
- 636 38. Slovitte R (1982) A simplified Timm stain procedure compatible with
637 formaldehyde fixation and routine paraffin embedding of rat brain. *Brain Res Bull*
638 8:771-774
- 639 39. Bancroft, JD, Gamble, M (2008) *Teory and Practice of Histological Techniques*, Reino
640 Unido: Churchill Livingstone 121-134.
- 641 40. McCormick N, Velasquez V, Finney L, Vogt S, Kelleher SL (2010) X-Ray
642 Fluorescence Microscopy Reveals Accumulation and Secretion of Discrete Intracellular
643 Zinc Pools in the Lactating Mouse Mammary Gland. *PLOS ONE* 5(6):e11078.
- 644 41. Klockenkämper R, Von Bohlen A (1996) Elemental analysis of environmental
645 Samples by total reflection fluorescence: a review. *X-Ray Spectrom* 25: 156-162
- 646 42. Takeda A (2001). Zinc homeostasis and functions of zinc in the brain. *BioMetals*
647 14:343-351.
- 648 43. Yokoyama M, Koh J, Choi DW (1986) Brief exposure to zinc is toxic to cortical
649 neurons. *NeurosciLett* 71:351-355.
- 650 44. Tubek S, Grzanka P, Tubek I (2008) Role of zinc in hemostasis: a review. *Biol*
651 *Trace Elem Res* 121:1-8
- 652 45. Suh SW, Jensen KB, Jensen MS, Silva DS, Kesslak PJ, Danscher G, Frederickson
653 CJ (2000). Histochemically-reactive zinc in amyloid plaques, angiopathy, and
654 degenerating neurons of Alzheimer's disease brains. *Brain Res* 852:274-278.

- 655 46. Person O, Botti AS, Péres MCLC (2006) Clinical repercussions of zinc deficiency in
656 human beings. *Arq Med ABC* 31:46-52.
- 657 47. Fluegge K BA. (2017). Zinc and Copper Metabolism and Risk of Autism: a reply to
658 Sayehmiri et al. *Iranian Journal of Child Neurology* 11(3), 66–69.
- 659 48. Kaur C, Ling EA (2017) The circumventricular organs. *Histol Histopathol*32(9):879-892.
- 660 49. Zatta P, Raso M, Zambenedetti P, Rocco P, Petretto A, Mauri P, Cozzi B (2006)
661 Metallothionein-I-II expression in young and adult bovine pineal gland. *J Chem Neuroanat*
662 31(2):124-129.
- 663 50. Zoroddu MA, Aaseth J, Crisponi G, Medici S, Peana M, Nurchi VM (2019) The essential
664 metals for humans: a brief overview. *J Inorg Biochem* 195:120-129.
- 665 51. Hock A, Demmel U, Schicha H, Kasperek K, Feinendegen LE (1975) Trace element
666 concentration in human brain. *Brain* 98:49-64.
- 667 52. Demmel U, Höck A, Kasperek K, Feinendegen LE (1982) Trace element concentration in
668 the human pineal body. Activation analysis of cobalt, iron, rubidium, selenium, zinc, antimony
669 and cesium. *Sci. Total Environ*24(2):135-146.
- 670 53. Takeda A (2004) Analysis of Brain Function and Preventions of Brain Diseases: the
671 actions of trace metals. *J Health Sci* 50(5), 429-44.
- 672 54. Cicero, CE, Mostile G, Vasta R, Rapisarda V.; Signorelli SS, Ferrante M, Zappia M,
673 Nicoletti A (2017) Metals and neurodegenerative diseases. A systematic review. *Environ Res*
674 159: 82–89.
- 675 55. Frederickson CJ, Suh SW, Silva D, Frederickson CJ, Thompson RB (2000)
676 Importance of zinc in the central nervous system: The zinc-containing neuron. *J Nutr*
677 130:1471S–1483S.
- 678 56. David J, Eide DJ (2006) Zinc transporters and the cellular trafficking of zinc. *Biochimica et*
679 *Biophysica Acta (BBA)Molecular Cell Research* 1763(7):711-722.
- 680 57. Palmiter RD, Cole TB, Quaife CJ (1996) ZnT-3 putative transporter zinc into synaptic
681 vesicles. *Proc Natl Acad Sci USA* 93:14934-14939
- 682 58. Kambe T, Taylor KM, Fu D (2021). Zinc transporters and their functional integration in
683 mammalian cells. *J Biol Chem* 296:1-27.
- 684 59. Weaver BP, Dufner-Beattie, J, Kambe, T, Andrews, GK (2007). Novel zinc-responsive
685 post-transcriptional mechanisms reciprocally regulate expression of the mouse Slc39a4 and
686 Slc39a5 zinc transporters (Zip4 and Zip5). *Biol Chem* 388, 1301–1312.
- 687 60. King, J. C., Shames, D. M., & Woodhouse, L. R. (2000). Zinc homeostasis in humans. *The*
688 *Journal of nutrition*, 130(5), 1360S-1366S.

- 689 61. Tubek, S. (2007). Zinc supplementation or regulation of its homeostasis: advantages and
690 threats. *Biological trace element research*, 119(1), 1-9.
- 691 62. Chung RS, West AK (2004) A role for extracellular metallothioneins in CNS injury and
692 Repair *Neurosci* 123:595-599.
- 693 63. Baltaci AK, Yuce K, Mogulkoc R (2018) Zinc Metabolism and Metallothioneins. *Biol*
694 *Trace Elem Res* 183(1):22-3.
- 695 64. Hongfang G, Guanghui C, Khan R, Huanxia J, Jianxin Z, Abbas Raza SH, Ayaz M, Shafiq
696 M, Zan L (2020) Review: Molecular structure and functions of zinc binding metallothionein-1
697 protein in mammalian body system. *Pak J Pharm Sci* 33(4):1719-1726.
- 698 65. Wan, Y, Zhang, B. (2022). The impact of zinc and zinc homeostasis on the intestinal
699 mucosal barrier and intestinal diseases. *Biomolecules*, 12(7), 900.
- 700 66. Kordas K, Stoltzfus RJ (2004) New Evidence of Iron and Zinc Interplay at the Enterocyte
701 and Neural Tissues. *J Nutr* 134: 1295–1298.
- 702 67. Grochowski, C, Blicharska, E, Krukow, P, Jonak, K, Maciejewski, M, Szczepanek, D,
703 Jonak, K, Flieger, J, Maciejewski, R (2019) Analysis of Trace Elements in Human Brain: Its
704 Aim, Methods, and Concentration Levels. *Frontiers in Chemistry*, 7.
705 <https://doi.org/10.3389/fchem.2019.00115>.
- 706 68. Kondaiah, P, Yaduvanshi, PS., Sharp, PA, Pullakhandam, R (2019). Iron and zinc
707 homeostasis and interactions: does enteric zinc excretion cross-talk with intestinal iron
708 absorption?. *Nutrients*, 11(8):1885.
- 709 69. Pereira AM, Maia MRG, Fonseca AJM, Cabrita ARJ (2021) . Zinc in Dog Nutrition,
710 Health and Disease: A Review. *Animals (Basel)*. 2021 Apr 1;11(4):978.
- 711 70. Maares, M., & Haase, H. (2020). A guide to human zinc absorption: General overview and
712 recent advances of in vitro intestinal models. *Nutrients*, 12(3), 762.
- 713 71. Liuzzi, JP, Bobo, JA., Lichten, LA., Samuelson, DA, Cousins, RJ (2004). Responsive
714 transporter genes within the murine intestinal-pancreatic axis form a basis of zinc
715 homeostasis. *Proceedings of the National Academy of Sciences*, 101(40), 14355-14360
- 716 72. Gupta, S, Merriman, C, Petzold, CJ., Ralston, CY, Fu, D (2019). Water molecules mediate
717 zinc mobility in the bacterial zinc diffusion channel ZIPB. *Journal of Biological*
718 *Chemistry*, 294(36), 13327-13335.
- 719 73. Thirumorthy, N, Manisenthil Kumar, KT., Shyam Sundar, A, Panayappan, L, Chatterjee,
720 M (2007). Metallothionein: an overview. *World journal of gastroenterology*, 13(7), 993–996.
721 <https://doi.org/10.3748/wjg.v13.i7.993>.

- 722 74. Hennigar, SR, Kelley, AM, McClung, JP (2016). Metallothionein and Zinc Transporter
723 Expression in Circulating Human Blood Cells as Biomarkers of Zinc Status: a Systematic
724 Review. *Advances in nutrition* (Bethesda, Md.), 7(4), 735–746.
725 <https://doi.org/10.3945/an.116.012518>
- 726 75.
- 727 76. Pup M, Ahmadi-Vincu M, Velcirov, AB, Gârban Z, Dronca, D (2006) The effect of zinc
728 chloride administration on some trace metals in Wistar rats liver. *J Agroalimnt Proc and*
729 *Technol XII*(2):521-528.
- 730 77. Himeno S, Fujishiro H. (2021) Roles of Zinc Transporters That Control the Essentiality
731 and Toxicity of Manganese and Cadmium. Cited in *Yakugaku Zasshi* 41(5):695-703. Japanese.
- 732 78. Qi Z, Liu KJ (2019) The interaction of zinc and the blood-brain barrier under physiological
733 and ischemic conditions. *Toxicol Appl Pharmacol* 364:114-119 .
- 734 79. Roohani, N, Hurrell, R, Kelishadi, R, & Schulin, R (2013). Zinc and its importance for
735 human health: An integrative review. *Journal of Research in Medical Sciences : The Official*
736 *Journal of Isfahan University of Medical Sciences*, 18(2), 144-157.
- 737 80. Mezzaroba, L, Alfieri, DF., Colado Simão, AN, Vissoci Reiche, EM. (2019). The role of
738 zinc, copper, manganese and iron in neurodegenerative diseases. *NeuroToxicology*, 74, 230-
739 241. <https://doi.org/10.1016/j.neuro.2019.07.007>
- 740 81. Barbier O, Jacquillet G, Tauc M, Cougnon M, Poujeol P (2005) Effect of Heavy Metals on,
741 and Handling by, the Kidney. *Nephron Physiol*;99:p105-p110. doi: 10.1159/000083981
- 742 82. Cousins RJ, Liuzzi JP, Lichten LA (2006) Mammalian zinc transport, trafficking,
743 and signals. *J Biol Chem*.281:24085–24089.
- 744 83. Kambe T, Tsuji T, Hashimoto A, Isumura N (2015). The physiological, biochemical, and
745 molecular roles of Zn zinc homeostasis and metabolism. *Physiol Rev* 96:749-784
- 746 84. Matsushima S, Reites RJ (1975) Ultrastructural observations of pineal gland capillaries in
747 four rodent species. *Am J Anat* 143:265-282.
- 748 85. Hodde KC, Veltman WA (1979) The vascularization of the pineal gland (epiphysis
749 cerebri) of the rat. *Scan Electron Microsc*. 1979;(3):369-74.
- 750 86. Duvernoy HM, Parratte B, Tatu L, Vuillier F (2000) The human pineal gland:
751 relationships with surrounding structures and blood supply. *Neurol Res*.22(8):747-90. doi:
752 10.1080/01616412.2000.11740753.
- 753 87. Sangiliyandi S, Quasim M, Kang MH, Kim JH, (2021): "Role and therapeutic potential of
754 melatonin in various type of cancers." *OncoTargets and therapy* 14:2019

- 755 88. Milatovic D, Zaja-Milatovic S, Gupta RC, Yu Y, Aschner M (2009) Oxidative damage and
756 neurodegeneration in manganese-induced neurotoxicity. *Toxicol Appl Pharmacol* 240:219-225.
- 757 87. Sangiliyandi S, Quasim M, Kang MH, Kim JH , (2021): "Role and therapeutic potential of
758 melatonin in various type of cancers." *OncoTargets and therapy* 14:2019
- 759 88. Milatovic D, Zaja-Milatovic S, Gupta RC, Yu Y, Aschner M (2009) Oxidative damage and
760 neurodegeneration in manganese-induced neurotoxicity. *Toxicol Appl Pharmacol* 240:219-225.
- 761 89. Taylor JG, Bushinsky DA (2009) Calcium and phosphorus homeostasis. *Blood Purif*
762 27:387-394.
- 763 90. Pozzan T, Rizzuto R (2000) The renaissance of mitochondrial calcium transport. *Eur J*
764 *Biochem* 267:5269-5273.
- 765 91. Santos APM, Milatovic D, Au C, Yin Z, Batoreu MC, Aschner M (2010) Rat brain
766 endothelial cells are a target of manganese toxicity. *Brain Res.* 1326:152-16.
- 767 92, Fujishiro H, Kambe T (2022) Manganese transport in mammals by zinc transporter
768 family proteins, ZNT and ZIP. *J Pharmacol Sci*148(1):125-133.
- 769 93. Gennari FJ (2002) Disorders of potassium homeostasis. Hypokalemia and hyperkalemia.
770 *Crit Care Clin* 18: 272-288.
- 771
- 772
- 773
- 774
- 775
- 776
- 777
- 778
- 779
- 780
- 781
- 782
- 783
- 784
- 785
- 786
- 787
- 788

789

790

791

792

793

794

795

796

797

798

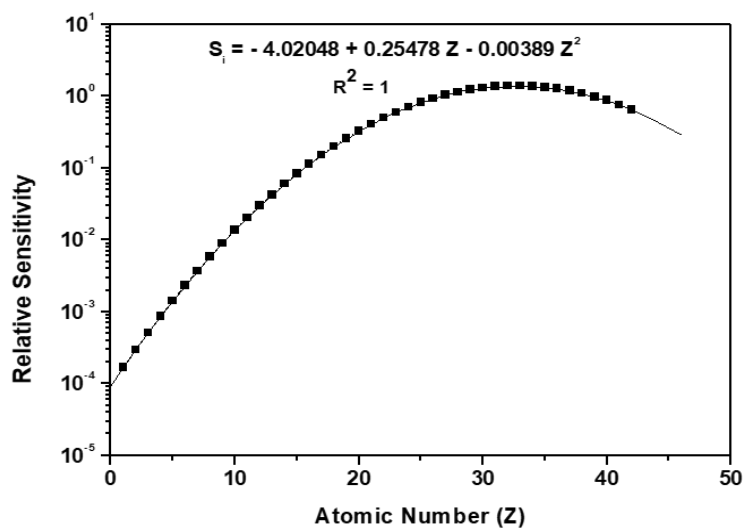
799

800

801

802

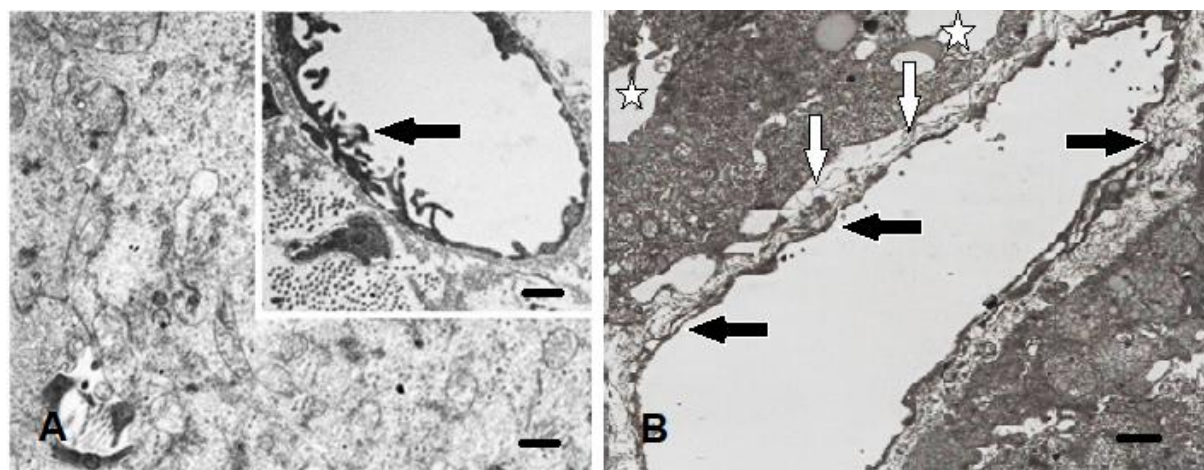
803 Supplementary information.



804

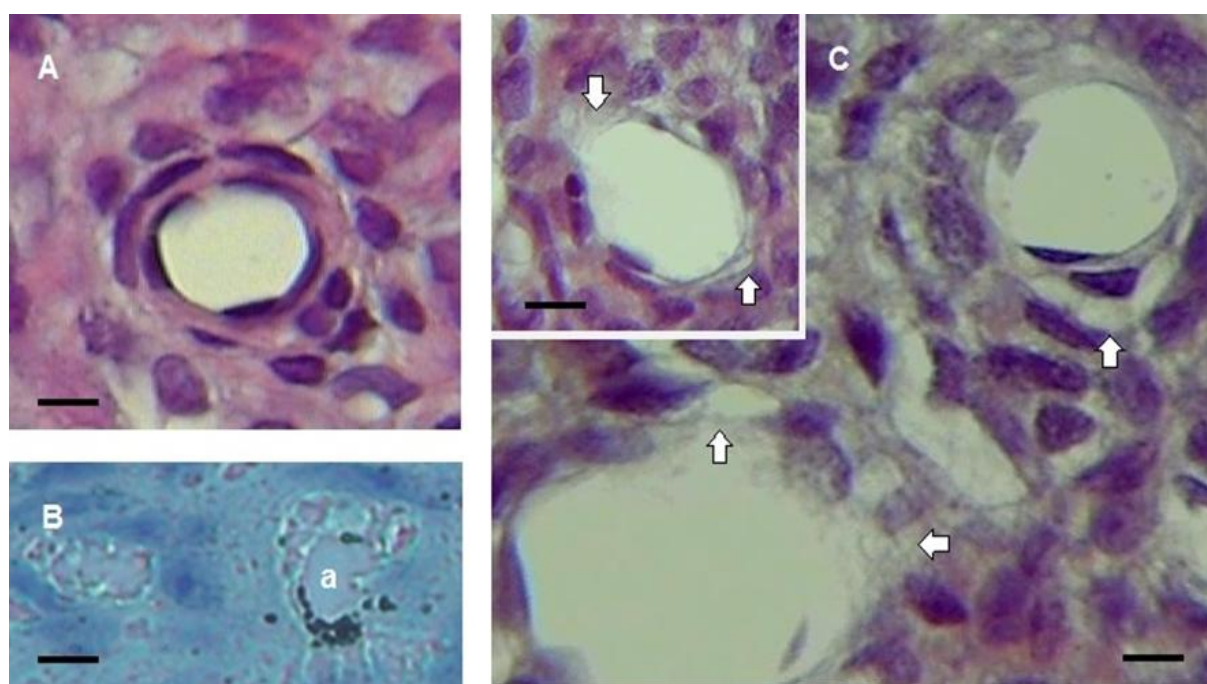
805 **Fig. 1** Calibration curve for the K-line elements using TXRF

806



807

808 **Fig. 2.** Electron micrograph of the pineal. Group CG (A) group EG (B). (A) The pineal
 809 parenchyma is homogeneous, and the intercellular spaces are much smaller. The insert in A
 810 represents a blood vessel where it is possible to observe the various fingers projections (black
 811 arrows) from the vessel wall to the lumen of this vessel. In the parenchyma (B) in the rat with
 812 excess Zn, the white arrows indicate areas where the architecture is not uniform, and appear
 813 to be extended with some arrangements fibrillar disorganized or absent fibrils. Many
 814 intercellular spaces seem enlarged. Changes can also be observed in the wall of blood vessels
 815 (black arrows in B) where a noticeable decrease in finger like projections, characteristic of
 816 normal pineal vessels can be observed and also the appearance of the walls is thinner and
 817 smoother and contain imperfections. Scale bar: 0.45 μ m.

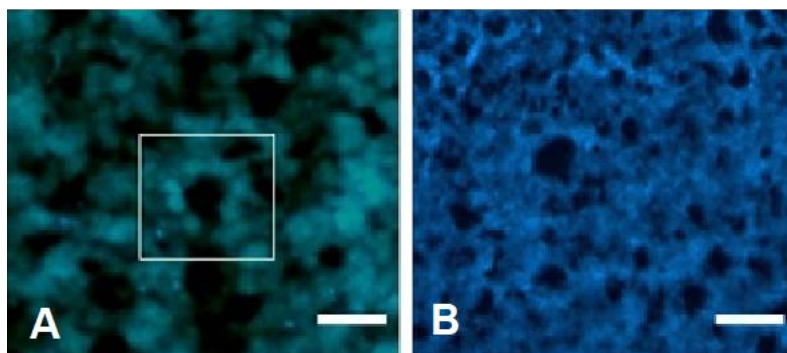


818

819

820 **Fig. 3.** Micrograph of parasagittal sections of the pineal glands. (A) in the control group (CG)
 821 showing a blood vessel stained by hematoxylin and eosin (HE) [39] with well-preserved wall.
 822 The peripheral parenchyma seem well organized. (B) Pineal gland from rats in the
 823 experimental group (EG). The Neo-Timm method revealed Zn aggregates (granulations in
 824 black) adjacent to blood vessels (a) seemingly in the perivascular space. Some pineal
 825 parenchymal cells (darker blue) had low visibility because of the need for more adjustments in
 826 the granulations of the over-focus peripheral area. (C) Experimental group (EG) pineal
 827 parenchymal (stained with HE) was not intact (white arrows in the insert) in contrast to the CG.
 828 This disruption (white arrows in C) was significant in relation to the blood vessel walls,
 829 sometimes in own wall the vessel other times were in the disorganized cytoarchitecture of the
 830 gland in various regions of the pineal parenchymal. Scale Bars: A,C, insert = 5.0 μm ;
 831 μm .

832
 833
 834
 835
 836
 837
 838
 839
 840



842 Fig. 4: A and B: Pineal gland treated by TSQ method. A: Sagittal sections of the pineal
 843 gland in animals treated with excess zinc (EG). Intense fluorescence of TSQ was observed in
 844 the pineal parenchyma and in the pseudo-rosette cells (demarcated area); B: Showing less
 845 evident fluorescence in the pineal parenchyma including the pseudo-rosette, with a lower
 846 degree of fluorescent labeling in the pinealocytes, and in these controls fluorescence is

847 considered to represent the location of zinc that normally exists in tissue; and Scale bar: 3,5
848 μm .